

For Reference

NOT TO BE TAKEN FROM THIS ROOM

INTERFEROMETER MEASUREMENTS OF THE
HYPERFINE STRUCTURE OF SOME SINGLY IONIZED
THALLIUM SPECTRAL LINES

by,

John Convey, B.Sc.

University of Alberta, 1936.


Ex LIBRIS
UNIVERSITATIS
ALBERTAENSIS





INTERFEROMETER MEASUREMENTS OF THE
HYPERFINE STRUCTURE OF SOME SINGLY IONIZED
THALLIUM SPECTRAL LINES

<u>Contents</u>	<u>Page</u>
1. Introduction.	1
2. The theory of Hyperfine Structure.	4
3. Experimental Procedure.	20
4. The Computation of the Wave Length Separations from the Interference Fringes produced by the Lummer Gehrcke Plate.	24
5. Method of measuring up the fringe pattern produced by Lummer Plates.	28
6. Experimental Results.	31
7. Discussion.	39
8. Acknowledgments.	49
9. References.	50



Digitized by the Internet Archive
in 2017 with funding from
University of Alberta Libraries

<https://archive.org/details/convey1936>

1. Introduction

Spectroscopic research, which has been so intensively pursued during the past thirty years or so, and which has provided such a wealth of information concerning the structure and mechanics of the atom, has until recently been mainly concentrated on the compilation of wave-length data, expressing the positions of spectral lines, and on the discovery and interpretation of regularities in these data. It is in this way that much of our knowledge of the arrangement of the electrons within the atom has been gained, and the majority of the more important atomic energy levels have been located.

According to the Quantum theory a given kind of atom possesses only certain discrete characteristic energy levels and when changing from higher to lower energy levels light is emitted whose wave length is inversely proportional to this energy difference. It is found that sometimes the spectral lines produced fall closely together in small groups, such as the two well known yellow sodium lines. Such structure is called fine, or multiple structure. Such fine structure is evidently due to small changes in wave length caused by small changes in energy differences. Thus we find groups of energy levels in the atom lying very close together.

However, lines which appear quite sharp in a spectrum obtained with a spectrograph of low dispersion,

when examined by apparatus of greater dispersive power such as a Fabry-Perot interferometer or a Lummer-Gehrcke plate, break up into a number of components. This is called Hyperfine structure. In terms of energy level diagrams hyperfine structure in a spectrum line is due to minute differences between energy levels of a group, attributed to the effect of the nucleus on the energy of the atom. However, experimental work has shewn that two types of hyperfine structure exist, one due to nuclear magnetic and mechanical moment, and a second due to isotope effects. In some elements hyperfine structure alone is observed, in others isotope structure alone is observed, and in still others both are observed.

Although there is yet much to be learned from an experimental and a theoretical standpoint, considerable progress has been made in the analysis and interpretation of hyperfine structure. Hence we might say the modern trend in spectroscopy is from the study of the macro-structure of Spectra to their micro-structure.

The term analysis of singly-ionized thallium over a region of $7,000 \text{ \AA}$ to $2,200 \text{ \AA}$ is fairly complete, and the magnitude of the hyperfine separations, together with the general simplicity of the patterns has resulted in quite a number of investigations. The spectrum of singly ionized thallium has been investigated by Rao,

Naryan and Rao (16), by McLennan, McLay and Crawford (17) and by Smith (18). A further analysis was done by McLennan, McLay and Crawford (19) and extended by Smith (20), not only increasing the number of known terms of singly ionized thallium but also revealing the fine structure character of some of the lines. Later, McLennan and Crawford (21) from an observation of the intensities and separations of the components of the hyperfine multiplets ^{gave} an interpretation of the hyperfine structure of singly ionized thallium, consistent with the F selection rule, the (JF) intensity rule, and the value $I = \frac{1}{2}$ for the nuclear moment, was deduced. Schüller and Keyston (22) observed the existence of isotope shifts in some of the hyperfine spectral levels of Tl, II. McLennan, McLay and Crawford (15) compared the numerical results, as shown on the previous paper (21) with the theory.

A further analysis of the hyperfine structure of singly ionized thallium is presented in this report.

See ELLIS + Sawyer Phys. Rev., Jan. 15th 1936 re. 160 new lines
classified in Tl.

Theory of Hyperfine Structure

The hyperfine structure of energy levels and spectral lines may be interpreted as the interaction of the nucleus of an atom and its surrounding electrons. In order to understand the origin of hyperfine structure of the spectra it is primarily necessary to have a clear understanding as to how fine structure multiplets arise.

Term Notation: The following notation is used :

l = the orbital quantum number.
 s = the electron spin quantum number.
 j = the inner quantum number, which
 is obtained by the vectorial
 addition of l and s , i.e. j may
 take the values $|l + s|, |l + s - 1|, \dots$
 $\dots, |l - s|$.

Different electrons possess different l values, taking any of the values 0, 1, 2, 3, 4, etc. For a given total quantum number n , the eccentricity of the orbit in which the electron moves depends on the value of l . Electrons for various l values are usually designated by the small letters s, p, d, f , etc., to which correspond the values $l = 0, 1, 2, 3$, etc. Atomic states corresponding to similar l values are designated by means of the capital letters S, P, D, F , etc. An atomic state is virtually a description of the energy and position of the optical electron, and the different states, or different energy values, which make up all the energy levels out of which the spectrum arises, are called terms. In describing

a term the j value is written to the right as a subscript, and the multiplicity of the term is written as a super-script on the left of the term designation. For example, consider the term $6s6p^3 D_3$, which indicates two valency electrons $6s$ and $6p$. We have a triplet D term with a j value equal to three.

When an electron is excited and lifted up to a high orbit, it tends to fall back to a lower orbit. The transitions allowed are subject to the selection principle that

$$\begin{aligned} \Delta j &= \pm 1 \text{ or } 0 \text{ with } j = 0 \rightarrow 0 \text{ forbidden} \\ \Delta \ell &= \pm 1. \end{aligned}$$

Fine Structure :

The study of the terms of a one electron atom, that is an atom with one valence electron such as, the alkalies, sodium, potassium, etc. is easily examined. However in discussion of spectra produced by atoms which have two or more valence electrons the task becomes more difficult; since the valence electrons interact with each other. Each of the valence electrons possess a spin angular momentum $\frac{sh}{2\pi}$ and an orbital angular momentum $\frac{\ell h}{2\pi}$ where ℓ may have any of the values 0, 1, 2, 3, 4, 5, etc. These vectors may combine in a variety of ways, and one may distinguish two extreme types of coupling called LS (Russell Saunders' coupling) and (jj)

respectively. In the vector notation small letters are used to represent specific angular momenta for individual electrons, and capital letters for resultant sums.

In L.S. coupling all the ℓ values form a resultant L and the s values a resultant S which then combine to form J . This simply means that when the interaction between different electrons of a configuration is very large compared with the interaction between the spins of each electron ^{and} ~~with~~ its own orbital motion, one speaks of Russell Saunders' coupling.

In (jj) coupling the ℓ and s of each electron combine to form a resultant j for each electron, and then all the j values form a resultant J . That is, when the interaction between the spin of each electron with its orbital motion is large compared with the interaction between the various electrons, one speaks of (jj) coupling.

The theory for fine structure shows that multiplet separations are due to the energy of interaction between the spin and orbital motions of the electrons (1). It can be shown that, in LS coupling, the interaction energy between the resultant angular orbital momentum L is given by E , when

$$E = A.LS. \overline{\cos. (SL)}.$$

where A = the interaction constant.

The interaction energy between two vectors is proportional to the cosine of the angle between these vectors, and it can be shown that the above expression is equivalent to :

$$E = \frac{A}{2} \left[J(J+1) - L(L+1) - S(S+1) \right] \quad \text{--- (1)}$$

This formula expresses the Landé Interval Rule, and from it the ratio of the intervals in a multiplet can be calculated. If the energy difference between two levels of the same multiplet is taken, one having a total moment J and the other $(J - 1)$; it can be seen that

$$E(J) - E(J - 1) = A \times J$$

The subsequent intervals are thus proportional to the larger value of J corresponding to one of the two adjacent levels. This simplified form of the Landé rule is true, for all cases in which strict LS coupling takes place. While the ratio of the intervals between the terms is a function of J , their actual separations depend upon the value of the interval factor A . This factor A depends upon the distance of the electron from the nucleus, the degree of penetration of the orbit, the screening effect of the other electrons, and the interaction energy between the electrons themselves. The interval factor, therefore, differs for different multiplets, usually diminishing as the orbital number of the optical electron increases.

Hyperfine Structure

Two types of hyperfine structure occur in line spectra and these arise from entirely different causes. The first type is due to the fact that the nuclei of atoms have the property of a spin. The other type is called the isotope type due the existence of isotopes.

Nuclear spin and Interaction of Nuclear and Electron Magnetic Moments

Associated with the nucleus we have a nuclear spin quantum number designated by I , the mechanical moment of momentum of the nucleus being $\frac{Ih}{2\pi}$. Goudsmit revealed that a new quantum vector, F , had to be added to the vector model of the atom (3). This vector F is the resultant obtained when the mechanical moment vector of the nucleus denoted by I is combined with the total mechanical moment vector J , of the extranuclear electrons. The different values of F correspond to the different hyperfine structure levels,

$$F = (I + J), (I + J - 1) \text{ ----- } (I - J).$$

The number of hyperfine structure levels is given by either $(2I+1)$ or $(2J+1)$ according to whether I or J is the smaller of the two. This rule shows that if the J values of a ^{level} ~~line~~ are known to be large, the nuclear spin may be determined directly from the number of lines ~~or levels~~ on the pattern. For allowed transitions between sets of levels the selection rules

for F in hyperfine structure are just the same as those for J in fine structure, viz.,

$$\Delta F = \pm 1 \text{ or } 0 \text{ with } F = 0 \rightarrow 0 \text{ forbidden.}$$

The separations in hyperfine structure are due to the interaction energy between the nuclear moment and the total extranuclear moment. The interaction energy between the two vectors I and J is dependent upon a number of factors. Firstly it is the value of the magnetic moment that determines the interaction energy of I and J . The nuclear magnetic moment $\mu = I \cdot g(I)$, so that $g(I)$ the nuclear constant is the ratio of the magnetic to the mechanical moment when quantum units are used. The second factor affecting the interaction energy is the nuclear charge, for the higher the degree of ionization the greater is the coupling energy between the extranuclear electron moment J and the nuclear spin I . A third factor is the eccentricity of the orbit of the optical electron. It can be seen that s-electrons will penetrate the inner shells to a greater extent than p-electrons, hence the coupling energy of an s electron will generally be much greater than that of a p-electron.

One-electron spectra

Calculations of the nuclear interaction with one valence electron have been made by Fermi (4) Casimir(5) Hargreaves(6) Breit(7) and Goudsmit(8).

The coupling between I and j may be considered as consisting of two parts. I couples with the orbital angular moment of the electron, that is (IL) coupling takes place, and I couples with the electron spin so that (IS) coupling also occurs. When these two effects are added the total interaction energy between nucleus and electron is obtained (9). The result shows that the energy E is given by the expression :

$$E = AIj \cos. (Ij) \dots\dots\dots(2)$$

which reduces to the form

$$E = \frac{A}{2} \left[F(F+1) - j(j+1) - I(I+1) \right] \dots(3)$$

This is identical with equation (1) if we replace F , j and I by J , L and S . Hence the Landé Interval rule holds for hyperfine structure, and this has been strongly supported by experimental observation. As an example consider the 6_1 term in the bismuth atom where $J=1$ and the observed value of $I = 9/2$. The allowed values of F are $11/2$, $9/2$ and $7/2$. According to the interval rule the difference between these levels should be in the ratio of 11 to 9, that is 1.222. The observed ratio of the intervals is 1.483 ^{to} ~~and~~ 1.214 which is 1.222, hence is in excellent agreement with the interval rule. (10)

The interval factor A can be approximately calculated for the simple case of one electron spectra. It is found that A is proportional to :

$$g(I) \frac{Z_i z^2}{n^3 (L + \frac{1}{2}) j(j+1)}$$

where Z_i and z are respectively the effective electric charges of the nucleus in the inner and outer portion of the penetrating orbit, and n is the effective quantum number.

Case of two s-electrons :

For more complex configurations, as an example consider two s-electrons, the interaction energy may be calculated completely in terms of each of the electrons. Casimir showed that in the particular case of an s-electron, the interaction energy is given by :

$$E = A I s. \cos. (I s).$$

Following Casimir, Goudsmit has calculated the interaction energy for an atom which has two valence s-electrons (9). If the subscripts denote the two electrons, the interaction energy is given by :

$$E = a_1 I s_1 \overline{\cos. (I s_1)} + a_2 I s_2 \overline{\cos. (I s_2)} \dots \dots (4)$$

Here a_1 and a_2 are the numerical proportionality factors for each electron respectively.

(4) reduces to an expression of the form

$$E = I j \cos. (I j) \left[\frac{a_1 s_1}{j} \cos. (s_1 j) + \frac{a_2 s_2}{j} \cos. (s_2 j) \right]$$

Comparing this with the previous expression equation (2)

$$E = A I j \cos. (I j)$$

Where $A = \frac{a_1 s_1 \cos(s, j)}{j} + \frac{a_2 s_2 \cos(s_2 j)}{j}$

This is found to reduce to the expression

$$A = a_1 \left[\frac{j(j+1) + s_1(s_1+1) - s_2(s_2+1)}{2j(j+1)} \right] + \frac{a_2 \left[j(j+1) + s_2(s_2+1) - s_1(s_1+1) \right]}{2j(j+1)} \dots\dots(5)$$

Since $s_1 = s_2 = \frac{1}{2}$, this reduces to

$$A = \frac{1}{2} a_1 + \frac{1}{2} a_2 \dots\dots\dots(6)$$

Experimental verification of this has been possible in a few cases. Thallium^{III} shows the interval factors for the hyperfine structures of the terms 6s 7s; 6s 9s, configurations:

An s-electron and a non-s-electron

In the case of an s-electron and an arbitrary other electron the evaluation of $a_1 s_1 \cos(I s_1)$ depends on the type of coupling of the quantum vectors of the extranuclear electrons. For Russell ^uSaunders coupling:

$$a_1 s_1 \cos(I s_1) = a_1 s_1 \cos(I j) \cos(j s) \cos(s s_1)$$

Where s represents the total spin momenta, and s_1 the spin moment of the s-electron. In this expression the interaction with the s-electron above is taken into account and the interaction with the other electrons is regarded as negligible.

$$a_1 s_1 \cos(I s_1) = I j \cos(I j) \left[\frac{a_1 s_1 \cos(s_1 s) \cos(s j)}{j} \right]$$

The expression in brackets is again the constant A

hence -

$$A = a_1 \left[\frac{s(s+1) + s_1(s_1+1) - s_2(s_2+1)}{2s(s+1)} \cdot \frac{j(j+1) + s(s+1) - l_2(l_2+1)}{2j(j+1)} \right]$$

In the case of two s electrons where $s_1 = s_2 = \frac{1}{2}$

$$A = a_1 \left[\frac{j(j+1) + s(s+1) - l_2(l_2+1)}{4j(j+1)} \right] \dots \dots \dots (7)$$

A can be expressed in terms of the Landé g-factor for the state under consideration.

$$A = \frac{a_1}{2} (g - 1) \dots \dots \dots (8)$$

For extreme (jj) coupling a similar treatment gives,

$$\begin{aligned} a_1 \cos. (is_1) &= a_1 \cos. (ij) \cos. (js_1) \\ &= ij \cos. (ij) \frac{a_1 s_1}{3} \cos. (js_1) \\ &= A. ij \cos. (ij) \end{aligned}$$

$$\text{where } A = a_1 \left[\frac{j(j+1) + s(s+1) - j_2(j_2+1)}{2j(j+1)} \right] \dots \dots \dots (9)$$

Here s_1 denotes the spin vector of the s-electron and s and j the resultant spin and the resultant extranuclear moment as usual. The quantum vectors of the second electron are denoted by the subscript 2. There exist relations between the values of A in the case of Russell Saunders coupling and in the case of (jj) coupling. These relations are similar to the well known sum rule of the Landé g values.

Expressions for hyperfine structure separations

of the levels of complicated electron configuration in different types of coupling have been deduced by Goudsmit (8). His method is that of the invariance of energy sums. Having considered the interaction of a magnetic nucleus and an electron in an s-state let us now consider the case of a non-s electron.

The method used by Goudsmit is as follows :

The interaction between the electrons is thought to be removed by the application of a fictitious very strong magnetic field, then each electron can be treated as independent of the others. Applying a magnetic field just uncouples the nuclear spin from the rest of the atom, giving each an independent projection on the field direction M_I and M_J . The interaction between the nucleus and the valence electron is given by

$$E = A(j) M_I M_J$$

A is the separation constant which governs the magnitude of the hyperfine multiplet of the particular level after the magnetic field is removed. The levels of the hyperfine multiplet are given by

$$E = A(j) I_j \cos. (I_j) \\ = \frac{A}{2} (j) \left[F(F+1) - I(I+1) - j(j+1) \right]$$

In the classical theory the interaction between a single non-s electron and a nuclear magnetic moment consists of two parts. The nuclear magnetic moment

is acted upon by a magnetic field caused by the orbital motion of the electron and also by a field produced by the electron spin. The expression for this interaction energy is (Ref: 3) page 50

$$E = E_l + E_s = a \left[I l \cos. (I l) - I s \cos. (I s) + 3 I s \cos. (I r) \cos. (r s) \right]$$

E_l and E_s represent the interaction energy due to the orbit^{al} motion of the valence electron and the spin of the electron respectively.

r -denotes the radius vector connecting the nucleus with the electron.

Neglecting all interactions between the quantum vectors and since the nuclear, the orbital and the spin moment have projections M_I , m_l and m_s respectively on the direction of the fictitious magnetic field and the vectors I , l and s will have independent Larmor precessions about the field direction the cosine terms of the preceding equation may be expanded. The resulting expression is

$$E = E_l + E_s = a M_I \left[m_l - m_s \frac{6m_l^2 - 2l(l+1)}{(2l-1)(2l+3)} \right] \dots \dots \dots (10)$$

This expression is valid only for non-s electrons.

The application of the sum rule and equation (10) to the case of a single electron provides a very simple derivation of the results obtained by Fermi, Casimir, Hargreaves and Breit using quantum mechanical methods. The resulting expression is

$$A(j) = \frac{a_{n\lambda} \ell(\ell+1)}{j(j+1)} \dots\dots\dots (11)$$

where $a_{n\lambda}$ is the interaction constant of an $n\lambda$ electron. The subscript "n" is the general designation for the principal quantum number of the electron and λ that for the orbital quantum number ($\lambda=0$ for s; 1 for p etc.)

For penetrating orbits other than those of s electrons $a_{n\lambda}$ is expressed approximately in cm^{-1} by,

$$a_{n\lambda} = \frac{R h c \alpha^2 Z_i Z_o^\lambda}{n_e^3 \ell(\ell+1)(\ell+\frac{1}{2})} g(I) \dots\dots\dots (12)$$

where Z_i and Z_o are the effective nuclear charges in the inner and outer part of the orbit respectively, n_e is the effective principal quantum number.

α = fine structure constant.

$g(I)$ = nuclear factor, given by the ratio between the nuclear magnetic moment in Bohr magnetons $\frac{eh}{4\pi mc}$ and the mechanical moment in units $\frac{h}{2\pi}$

Hyperfine structure for extreme (jj) coupling

In LS. coupling it is only possible to give the sum of the interval factors for all the terms of a multiplet group which have the same J value. For example, the D terms which arise from an sd electron configuration are 3D_2 , 3D_1 , 3D_0 , and 1D_2 . The interval factors for the 3D_1 and 3D_2 terms can be calculated, but only the sum of the interval factors for the two terms 3D_2 and 1D_2 is obtained

since they have identical j values.. For spectra which show (jj) type of coupling the interval factor for every term is given separately.

When the spin and orbit of an electron are coupled, the interaction with the nuclear magnetism is given as

$$E = a_1 I j_1 \cos. (I j_1) \text{ or } a_2 I j_2 \cos. (I j_2)$$

where a_1 or a_2 depends on whether one considers the state with $j_1 = \ell + \frac{1}{2}$ or the one with $j_2 = (\ell - \frac{1}{2})$. For several electrons the total interaction with the nucleus is

$$E = \sum a_k I j_k \cos. (I j_k) \dots\dots\dots (13)$$

Goudsmit (8) has shown expression (13) reduces to one of the form,

$$E = A I J \cos. (I J)$$

where $A = \sum a_k \frac{j_k}{J} \cos. (J j_k)$

Considering the case of equivalent electrons, it can be

$$\text{shown that } A = a_1 \frac{g_1 - g_2}{g_1 + g_2} + a_2 \frac{g_2 - g_1}{g_1 + g_2}$$

where the values of g_1 and g_2 are the known g values for a single electron, the values of g to be used are those for the extreme (jj) , coupling of the configuration under consideration.

The addition of a single s electron to a state for which A is known results in the following expression,

$$A = A^+ \left[\frac{J(J+1) + J^+(J^++1) - s(s+1)}{2J(J+1)} \right] + \langle p, \pi \rangle$$

$$+ b \left[\frac{J(J+1) + s(s+1) - J^+(J^++1)}{2J(J+1)} \right] \dots\dots\dots(14)$$

A^+ and J^+ are the values of the state to which the s-electron is added.

b and s characterize the s-electron.

A and J denote the final level.

?

Isotope Effect

Besides hyperfine structure due to a nuclear magnetic and mechanical moment, a second hyperfine structure due to the different isotopes of the same chemical element is also found. Hyperfine structure is observed only in the cases of isotopes with odd mass number, since isotopes with even mass number have either a zero mechanical moment or zero magnetic moment. In elements such as mercury and Thallium where isotope structure is present, it is found that relative shifts of a set of terms belonging to one isotope are practically the same as the relative shifts of the same levels in another isotope. Because there are no combinations between the levels of one isotope and those of another, one cannot say how much one system has been shifted from the other, but only how levels shift relative to others. The relative shifts where observed are found to be approximately proportional to the mass differences. The suggestion that isotope shift may be due to a change in the Rydberg constant

is occasionally but not always in agreement with experiment. Attempts to calculate isotope displacements in heavy elements have been made by Breit. These calculations, based upon a change in the size of the nucleus, are in fair agreement with the relative shifts observed in mercury, thallium and lead.

Experimental Procedure

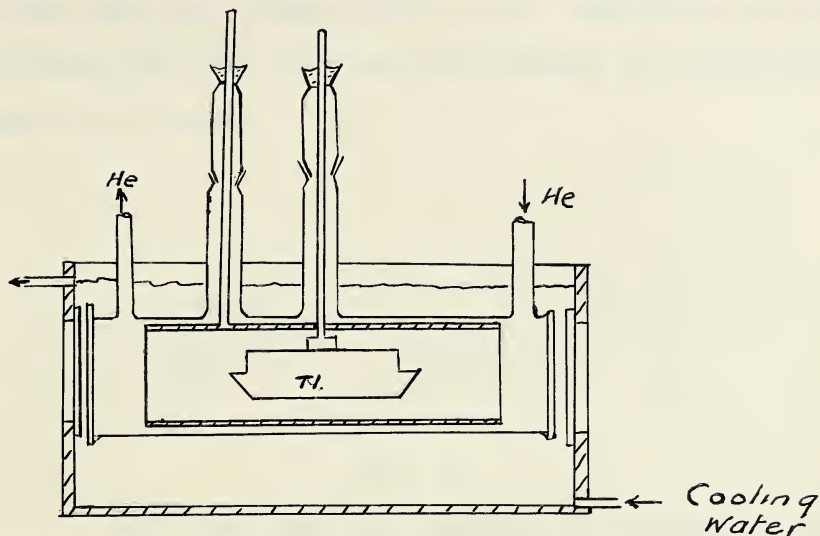


Fig. 1

The source S, fig. (2) was Thallium in a water-cooled hollow cathode discharge in an atmosphere of helium at a pressure of about 0.7 cm., of Hg. The arrangement is shown in fig. (1). The pyrex glass tube of length 30 cms. and internal diameter 4.6 cms. had an aluminium anode and a molybdenum cathode of length 7 cms. and a diameter of 1.7 cms. The helium was circulated through the discharge tube by means of two mercury pumps in tandem and cleaned by passing through charcoal immersed in CO_2 snow. The relatively high pressure of helium was used to keep the Thallium vapour from diffusing out of the cathode. Both the pyrex tube and water bath were provided with quartz windows to let through the ultra-violet light.

The discharge was excited by applying a voltage of about 800 volts supplied by a D.C. generator in series with about 900 ohms., the current through the tube being normally 0.24 amps.

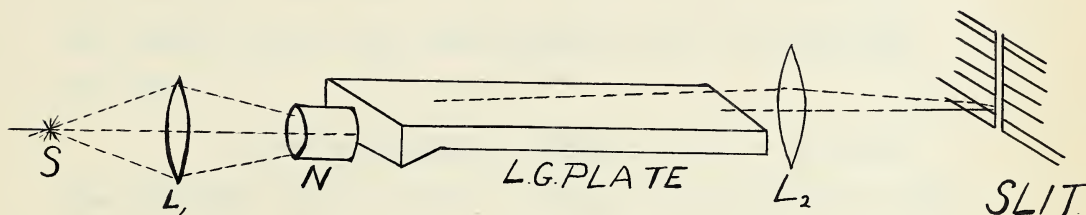


Fig. 2

The light from the cathode was condensed on to the reflecting prism of the Lummer Gehreke plate by means of a quartz lens L_1 , and the fringes formed were focussed on the slit of a Hilger, E_1 Spectrograph by a quartz fluorite lens of focal length 23 cms. The plane of the Lummer plate was horizontal, i.e. perpendicular to the slit of the spectrograph.

The Lummer plate, its adjustable holder, and Nicol prism, in the case of the quartz plate, were housed in a double-walled box made of "ten-test", the windows of which were formed by the quartz condensing lens L_1 , and the quartz fluorite projecting lens L_2 , the latter being rigidly attached to the spectrograph. The interferometer system and the spectrograph stood on a rigid steel plate. The discharge tube, circulating pumps, purifying tubes and helium reservoirs, formed a

complete unit rigidly attached to the top of a table of adjustable height. The whole system travelled on wheels along a track permitting the maintenance of the alignment of the tube with the optical system. Hence the relative position of the source with respect to the Lummer plate and spectrograph could be adjusted at will.

Since temperature changes tend to broaden the spectral lines due to a change in thickness of the Lummer plate, also changing refractive indices of the plate, it was essential to maintain the temperature of the spectrograph and the interferometer as constant as possible, especially when long exposures of ten hours' duration or more were made. For this purpose two mercury contact thermostats were used. One of these kept the room temperature constant with a maximum variation of about 0.5° C, and the other maintained the temperature of the box constant. The amplitude of the variation of the air temperature in the box being about 0.2° C, the temperature changes in the Lummer plate itself would probably be less than this.

Two glass Lummer plates of length 13 and 20 cms., with respective thicknesses 0.4872 and 0.6176 cms. and two quartz Lummer plates of length 13 cms., and respective thicknesses 0.4493 cms. and 0.5872 cms. were used. The optic axis of the 4 m.m. quartz Lummer plate was parallel to the long edge of the

plate, while the 6 m.m. quartz plate had its optic axis at right angles to the long edge. A nicol prism with its short diagonal horizontal was inserted between the condensing lens and plate, so that the light travelled through the plate as ^{the} ordinary ray in the 4 m.m. quartz plate, and as the extraordinary ray for 6 m.m. plate.

The Lummer plate was always adjusted to give simultaneously the fringes from both the top and bottom of the plate. The adjustment of the angle of incidence of light on the reflecting prism of the Lummer plate to obtain symmetry between the two sets of fringes was found to be very critical.

For the shorter wave length region that is the violet and ultra-violet region Eastman 33 plates were used and Process panchromatic plates for the larger λ regions. The photographic plates were developed by means of Agfa-fine grain developer and fixed with a special acetic acid fixing solution. The fringes were measured on a comparator.

The Computation of the Wave Length Separations
from the Interference Fringes produced by the
Lummer Gehreke Plate.

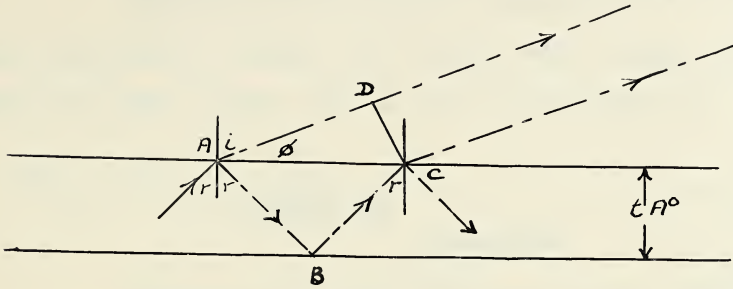


Fig. 1

The above figure represents a side view of the interferometer with typical rays passing through it.

From the figure we see that the retardation q between AD and ABC is

$$\begin{aligned}
 q &= AB + BC - AD \\
 &= 2 (\mu t \sec r) - 2(t \tan r) \sin i \\
 &= 2 t \cdot (\mu / \cos r - \mu \sin^2 r / \cos r) \\
 &\quad \text{since } \mu = \sin i / \sin r \\
 &= 2 t \mu \cos r \\
 &= 2 t \sqrt{\mu^2 - \sin^2 i}
 \end{aligned}$$

The condition for bright fringes is that $q = n \lambda$ where n is a positive integer.

$$n \lambda = 2 t \sqrt{\mu^2 - \sin^2 i} \dots \dots \dots (1)$$

Squaring (1) and differentiating with λ constant,

$$n \cdot \lambda^2 \cdot \delta n = -4 t^2 \sin i \cos i \cdot \delta i$$

$$\delta i = \frac{-n \lambda^2}{2 t^2 \sin 2i} \delta n \dots \dots \dots (2)$$

$\lambda \text{ CONSTANT.}$

or by (1)

$$\delta i = \frac{-\lambda \sqrt{\mu^2 - \sin^2 i}}{t \sin 2i} \frac{1}{\lambda \text{ constant}} \delta n \dots \dots \dots (3)$$

Therefore the angular separation δi , between two consecutive orders of a given wave length is obtained from either (2) or (3) by putting $\delta n = 1$.

$$\delta i_1 = -\delta \phi_1 = \frac{-n \lambda^2}{2 t^2 \sin 2i} \dots \dots \dots (4)$$

$\lambda \text{ constant}$

Squaring (1) and differentiating partially with respect to λ ,

$$n^2 \lambda = 2 t^2 (2 \mu \frac{\partial \mu}{\partial \lambda} - \sin 2i \frac{\partial i}{\partial \lambda})$$

$$\frac{\delta i}{\delta \lambda} = \frac{4 t^2 \mu \frac{\partial \mu}{\partial \lambda} - n^2 \lambda}{2 t^2 \sin 2i} \dots \dots \dots (5)$$

$n \text{ constant}$

Consider now two wave lengths λ and λ' the latter being slightly the longer. Suppose that the difference in wave lengths is such that for a given interferometer plate and near grazing emergence a fringe of wave length λ' and order n coincides with a fringe of wave length λ and order $n+1$. Let us denote this wave length difference by $\delta \lambda$. Placing this value of $\delta \lambda$ in equation (5) we must get the same value for δi as we obtained from equation (4) for successive orders. Thus dividing (5) into (4) we find :

$$\delta \lambda_1 = \frac{n \lambda^2}{n^2 \lambda - 4 t^2 \mu \frac{\partial \mu}{\partial \lambda}} \dots \dots \dots (6)$$

$$= \frac{\lambda^2 \sqrt{\mu^2 - 1}}{2 t (\mu^2 - 1 - \lambda \mu \frac{\partial \mu}{\partial \lambda})} \dots \dots \dots (7)$$

by substituting for n from (1) and since $i = \pi/2$ near grazing emergence.

The values of μ and $\frac{d\mu}{d\lambda}$ are obtained from equations (8), (9) and (10) to follow.

Drude's equation for the Index of Refraction of the Ordinary Ray in Quartz (11)

$$\mu_{\lambda}^2 = b^2 + \sum_{k=1}^3 \frac{M_k}{\lambda^2 - \lambda_k^2} \dots \dots \dots (8)$$

where

μ_{λ} = the refractive index for the wave length λ
 λ = the wave length in Angstroms.

The constants are as follows :-

$$b^2 = 4,5800$$

$$M_1 = 1.06 \times 10^6 \quad \lambda_1^2 = 106 \times 10^4$$

$$M_2 = 4.4224 \times 10^9 \quad \lambda_2^2 = 782,200 \times 10^4$$

$$M_3 = 7.1355 \times 10^{10} \quad \lambda_3^2 = 4,305,600 \times 10^4$$

Differentiating (8) we have,

$$\frac{d\mu}{d\lambda} = - \frac{\lambda}{\mu} \sum_{k=1}^3 \frac{M_k}{(\lambda^2 - \lambda_k^2)^2} \dots \dots \dots (9)$$

Hence substituting in equation (7) we have :

$$t \delta \lambda = \frac{\lambda^2 \sqrt{\mu^2 - 1}}{2 \left[\lambda^2 - 1 + \lambda^2 \sum_{k=1}^3 \frac{M_k}{(\lambda^2 - \lambda_k^2)^2} \right]} \dots \dots \dots (10)$$

For the extraordinary ray and in the case of the glass Lummer plates the Cauchy formula was used, namely :

$$\mu = C + D/\lambda^2$$

$$d\mu/d\lambda = -2D/\lambda^3$$

hence substituting in equation (7) for $\frac{d\mu}{d\lambda}$ we have :

$$2t.\delta\lambda = \frac{\lambda^2 \sqrt{\mu^2 - 1}}{\left[(\mu^2 - 1) + 2 \frac{D\mu}{\lambda^2} \right]} \dots\dots\dots(11)$$

Now $\nu = 1/\lambda$

$$\text{hence } d\nu = - \frac{d\lambda}{\lambda^2}$$

Hence substituting for $d\lambda$ in equation (11) we have

$$2t.d\nu = \frac{-\sqrt{\mu^2 - 1}}{\left[(\mu^2 - 1) + 2 \frac{\mu D}{\lambda^2} \right]}$$

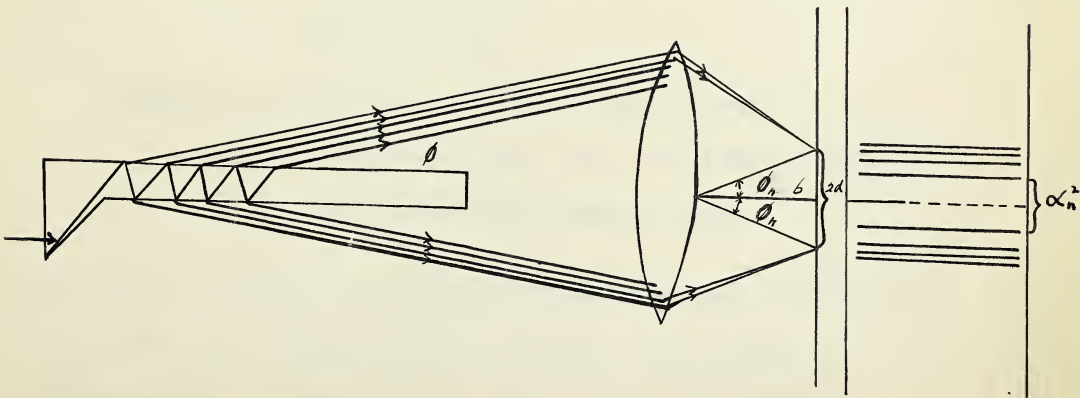
The foregoing equations were used to calculate the wave number separations for the various wave lengths, and particular plates. The results obtained were plotted and found to lie on smooth curves of wave number separation against wave length.

Method of Measuring up the fringe pattern produced
by Lummer plate.

To carry out the analysis the procedure is as follows :

The fringes produced by plates of different thicknesses are photographed in succession, the coarse structure being dispersed in a horizontal direction by a prism spectrograph_{with wide slit}, and the hyperfine structure vertically by means of the interferometer. We thus obtain on the photographic plate wide images of the slit corresponding to the spectral lines, which are crossed by the horizontal fringes of the hyperfine structure.

A precise method of measuring the photographic fringe patterns produced by Lummer plates is due to McLennan and McLeod (12), in which the geometrically central line of the double fringe patterns is taken as the line of reference in the measurements. This exact formula permits of the use of the fringes that emerge from the plate at nearly grazing direction, for which the dispersion is the greatest.



From the figure we find $i = \frac{\pi}{2} - \phi$ -----

and from the theory of the Lummer Plate we find :

$$n\lambda = 2t \sqrt{\mu^2 - \cos^2 \phi} = 2t \sqrt{\mu^2 - 1} \quad (\text{approx.})$$

Since ϕ is small, $\cos \phi = 1 - \phi^2/2$

$$\text{then } n\lambda = 2t \sqrt{\mu^2 - (1 - \phi^2/2)} = 2t \sqrt{\mu^2 - 1} \left(1 + \frac{1}{4} \frac{\phi^2}{\mu^2 - 1}\right) \dots (1)$$

neglecting ϕ^4 and higher terms.

$$\text{Similarly } (n+1)\lambda = 2t \sqrt{\mu^2 - 1} \left(1 + \frac{1}{4} \frac{\phi_{n+1}^2}{\mu^2 - 1}\right) \dots (2)$$

Subtracting (1) and (2)

$$\begin{aligned} \lambda &= 2t \sqrt{\mu^2 - 1} \left(\frac{1}{4}\right) \frac{1}{\mu^2 - 1} [\phi_{n+1}^2 - \phi_n^2] \\ &= \frac{t}{2\sqrt{\mu^2 - 1}} (\phi_{n+1}^2 - \phi_n^2) \dots (3) \end{aligned}$$

Equation (3) thus refers to the angular separation of two consecutive orders of λ .

In measuring a plate ϕ cannot be measured directly but the distance 2α shown in the figure can be determined. Now 2α is directly proportional to 2ϕ i.e. since ϕ is small $2\alpha/b$ equals 2ϕ .

Thus the fringes constituting any one set are spaced according to

$$\lambda = \frac{t}{2b^2} \frac{[\alpha_{n+1}^2 - \alpha_n^2]}{[\mu_\lambda^2 - 1]^{1/2}}$$

where t = thickness of the Lummer plate.

μ_λ = refractive index for the wave length λ .

b = focal length of camera lens.

$2\alpha_1, 2\alpha_2, \dots, 2\alpha_n$ the distances between the centres of the main line fringe taken in pairs, one being on either side of the central line of the photograph.

Denoting $\alpha_{n+m}^2 - \alpha_n^2 = N_m$

and $\alpha_{n+1}^2 - \alpha_n^2 = N_1$

we have for the whole pattern $\frac{N_m}{m} = N_1$

$$\text{so } m\lambda = \frac{t [\alpha_{n+m}^2 - \alpha_n^2]}{2b^2 (\mu^2 - 1)^{1/2}}$$

The difference between the wave lengths of the different satellites, and the wave length of the main constituent is obtained from the equation :

$$\Delta\lambda = \frac{\delta(\alpha^2) \cdot \Delta\lambda_m}{N_1}$$

$$\text{where } \Delta\lambda_m = \frac{n\lambda^2}{n^2\lambda - 4t^2\mu \frac{d\mu}{d\lambda}}$$

$$n = \frac{2t\sqrt{\mu^2 - 1}}{\lambda}$$

$$\delta(\alpha^2) = \alpha_s^2 - \alpha_m^2$$

where α_m = the distance of a main line fringe from the central line of the pattern.

α_s = distance from the central line of a satellite fringe of the same order as α_m

Thus the formula may be written as :

$$\Delta\lambda = \frac{\alpha_s^2 - \alpha_m^2}{\alpha_m^2 - \alpha_{m,1}^2} \Delta\lambda_m$$

In terms of wave number separation we have :

$$\Delta\lambda = \frac{\alpha_s^2 - \alpha_m^2}{\alpha_m^2 - \alpha_{m,1}^2} \Delta\lambda_m$$

where $\alpha_{m,1}$ is the distance of the next higher order.

Experimental Results

The observations and results of this investigation are presented in the following pages. The line spectra for thallium was obtained for the range of approximately 7,000 Å to 3,000 Å.

An interpretation of the hyperfine structure patterns obtained, was as follows. The transitions allowed between hyperfine multiplets were calculated according to the selection rules $\Delta f = \pm 1$ or 0. In most cases investigated all of the expected components were not found. The relative intensities of the expected hyperfine components were calculated by means of the intensity formulae derived by Hill (14) and these intensities compared with the observed intensities, thus enabling us to recognise the various components. However, on some of the plates, the lines of the hyperfine pattern were found to overlap, while on other patterns, more than the expected number of components were found due to isotope shifts of the energy levels.

5183 Classification $6s5f^3F_3$ - $6s6d^3D_3$

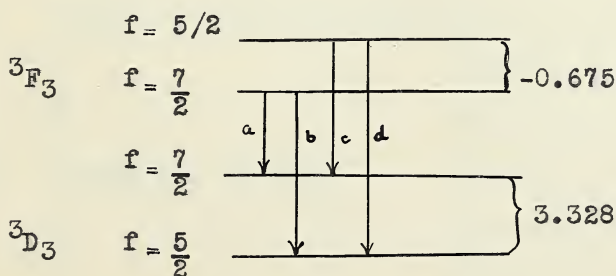
According to the theory of hyperfine structure four components are expected for this pattern. Only two components were observed, with a very faint trace of a third component, when the 4 m.m. quartz Lummer plate was used. Table I presents the observations obtained. The first column indicates how the components originate; e.g. d arises from a transition

from the $f = 5/2$ level of 3F_3 to the $f = 5/2$ level of 3D_3 . The second column gives the theoretical intensities calculated by the formulae of Hill.

Table 1			Observed $\Delta\nu$ cms.-1			
Changes in f	Theoretical Intensity	Designation of Component	G.4 No.1	G.4 2	Q.4 1	G.6 1
$\frac{7}{2} \longrightarrow \frac{7}{2}$	100	a	0	0	0	0
$\frac{5}{2} \longrightarrow \frac{7}{2}$	3.7	c	-	-	-	-
$\frac{7}{2} \longrightarrow \frac{5}{2}$	3.7	b	-	-	-	-
$\frac{5}{2} \longrightarrow \frac{5}{2}$	74	d	3.999	3.999	4.008	4.007

The fourth column indicates the particular plate measured. G.4 plate No.1 means the 4 m.m. glass Lummer plate, G.6 means the 6m.m. glass Lummer plate, and Q.4 is the quartz Lummer plate of thickness 4 m.m.

Schüler investigated and found the level $6s5f\,{}^3F_3$ had a separation of -0.675 cms.⁽¹²⁾ The hyperfine energy level diagram for this particular transition is as follows :



Therefore having observed the separation of the two

strong components a and d on several plates and accepting Schüller's value of -0.675 cms.^{-1} for the 3F_3 level separation, then the separation of the 3D_3 level is obtained.

Procedures similar to this were adopted for the other level separations obtained. The following table II contains a summary of the results which were found. In the first column is the approximate wave length of the line examined and the classification is given in column two. Column three gives the level whose separation is under investigation, the separation being shown in column five. Column four indicates the particular plate measured, using the same symbols as expressed in table I.

Table II

λ approx. in A	Classification	Term	Plate	Hyperfine Structural Interval in cms.^{-1}
5183	$6s5f^3F_3 - 6s6d^3D_3$	$6s6d^3D_3$	G4 No.1	3.324
			Q4 No.1	3.333
			G6 No.1	3.332
			G4 No.2	3.324
				<u><u>$3.328 \pm .004$</u></u>
3364	$6s6d^3D_3 - 6s6f^1F_3$	$6s6f^1F_3$	Q6 No.1	2.955
			Q4 No.1	2.948
			Q4 No.2	2.958
3320	$6s6d^3D_2 - 6s6f^1F_3$		Q4 No.1	2.961
			Q4 No.2	2.958
			Q6 No.1	2.948
				<u><u>$2.955 \pm .004$</u></u>

$\lambda_{\text{approx.}}$ in Å	Classification	Term	Plate	Hyperfine Structural Interval in cms. ⁻¹
3321	$6s6d^3D_2 - 6s6f^3F_3$	$6s6f^3F_3$	Q4 No.1	2.283
			Q6 No.1	2.288
			Q6 No.2	2.276
3365			Q6 No.1	2.287
			Q4 No.1	2.289
			Q4 No.2	2.285
				$2.285 \pm .003$
3291	$6s6d^3D_1 - 6s6f^3F_2$	$6s6f^3F_2$	Q4 No.1	-2.778
			Q4 No.2	-2.772
3322			Q6 No.1	-2.786
				$-2.779 \pm .004$
3369	$6s6d^3D_3 - 6s6f^3F_4$	$6s6f^3F_4$	Q4 No.1	3.518
			Q6 No.1	3.523
			Q4 No. 2	3.518
			Q6 No.2	3.523
				$3.521 \pm .003$
6181	$6s7p^3P_2 - 6s7d^3D_3$	$6s7d^3D_3$	Q6 No.1	3.380
			Q4 No.1	3.378
			G6 No.1	3.368
			G4 No.1	3.368
				$3,374 \pm .005$

λ approx. in Å	Classification	Term	Plate	Hyperfine Structural Interval in cms. ⁻¹
4274	$6s7p^3P_2 - 6s9s^3S_1$	$6s9s^3S_1$	Q4 No.1	4.546
			Q4 No.2	4.546
			Q4 No.3	4.546
			Q6 No.1	4.556
			Q6 No.2	4.555
3837	$6s7p^3P_0 - 6s9s^3S_1$	$6s9s^3S_1$	Q4 No.1	4.548
			Q4 No.2	4.545
			Q4 No.3	4.540
			Q6 No.1	4.554
			Q6 No.2	4.553

$6s6f^1F_3$

This particular level was investigated by means of the two lines 3364 and 3320. In the case of the line 3364, only two of the components were resolved and the pattern obtained was mixed with that of the line 3365. However, the separation of the components of these two transitions were found respectively.

Using the separation value which was obtained for the $6s6d^3D_3$ level, the value of the $6s6f^1F_3$ level was found.

The line 3320 is one of the triplet, 3320, 3321 and 3322, hence the pattern obtained in this case was very complex. Nine components were found, although three of these components could not be measured throughout the whole of the patterns obtained.

Each of the lines of this triplet involved the level $6s6d^3D_2$ which had been measured by Schuler⁽¹¹⁾ hence the determination of the separation of the other respective levels could be found. In the case of the line 3320 a value of the separation for the level $6s6f^3F_3$ was found.

$6s6f^3F_3$

The separation of this level was obtained from the lines 3321 and 3365, whose particular hyperfine patterns have already been mentioned. The line 3365 involved the level $6s6d^3D_3$.

$6s6f^3F_2$

This level was examined by means of the lines 3291 and 3322. The hyperfine pattern for the line 3291 revealed two components. The separation between these components was found and using Schuler's value of -2.121 cm^{-1} for the $6s6d^3D_1$ level the separation for $6s6f^3F_2$ was determined.

$6s6f^3F_4$

The separation of this level was determined by an examination of the line 3369. Only two components were resolved, and their separation was found. Knowing the separation of the $6s6d^3D_3$ level the separation of the $6s6f^3F_4$ level was found.

$6s7d^3D_3$

An examination of the line 6181 yielded the separation of the level $6s7d^3D_3$. Only two components were resolved. Schuler's value of 3.472 for the $6s7p^3P_2$ level was used in the derivation of the result.

$6s9s^3S_1$

The investigation of this level was done by means of the two lines 4274 and 3837. Of the four components expected for the 4274 classification, only two were resolved. Taking Schüller's value of 3.472 cms.^{-1} for the $6s7p^3P_1$ level which occurs in this transition the separation of the $6s9s^3S_1$ level was determined.

Since the classification of the line 3,837 is $6s7p^3P_0 - 6s9s^3S_1$, the level 3P_0 has no hyperfine splitting and only two hyperfine components are expected. Hence the hyperfine separation of the level $6s9s^3S_1$ was determined directly.

This level separation was measured by Mr. Smith using the line 3869 whose classification is $6s7p^3P_1 - 6s9s^3S_1$. The four components as expected were all resolved on four plates, two were very strong but the others were weak although measurable. Hence measurements of the hyperfine separations of both the $6s9s^3S_1$ and $6s7p^3P_1$ levels were obtained. The observed values were 4.550 cms.^{-1} for the $6s9s^3S_1$ level, and 4.000 cms.^{-1} for the $6s7p^3P_1$ level separation.

From a consideration of the observed separations of the terms as shown in table II, the interaction coefficient A may be determined. The results are summarized in the following table ;

Configuration	Term	observed Δv cm ⁻¹	Λ cm ⁻¹
6s6d	³ D ₃	3.328	0.951
	³ D ₂	0.555 (S)	0.222
	³ D ₁	-2.121	-1.414
6s7d	³ D ₃	3.374	0.964
	³ D ₂	0.78 (C)	0.31
	³ D ₁	5.88 (C)	-1.47
6s6f	³ F ₄	3.521	0.782
	³ F ₃	2.285	0.653
	³ F ₂	-2.779	-1.112
	³ F ₃	2.955	0.844
6s9s	³ S ₁	4.549	3.003
6s7s	³ S ₁	4.980 (S)	3.320

(S) - Schuler's value. ref.(22)

(C) - Crawford's value. ref. (21)

Discussion:-

Thallium is the element of atomic number 81, possessing two isotopes of atomic weights 203 and 205, and occupying a position in the sixth row, third column of the periodic table of the elements. Singly ionized thallium is a two electron system hence the general theory developed by Goudsmit, can be applied in the interpretation of its hyperfine structure. The following discussion will deal with the application of both (SL) coupling, and (jj) coupling to several terms.

(SL) coupling

(a) 6s6d

sd electronic configurations give rise to four spectral states, represented as 3D_3 , 3D_2 , 1D_2 and 3D_1 . Applying the sum rules, the interval factors $A(^3D_3)$ and $A(^3D_1)$ are determined in terms of the two interaction constants b and a which represent the 6s and nd electrons respectively. Only the sum of $A(^1D_2)$ and $A(^3D_2)$ is expressed in terms of the constants b and a. The formulae, together with the observed values of the interval factors of the states of these configurations are listed in tables I, II and III, in the third column is the value of b deduced by neglecting the value of a.

(C) = Crawford's value, (S) = Schuler's value.

6s6d

Table I

Formula	Observed Interval Factors	b cms ⁻¹
(1) $A(^3D_3) = b/6 + 4/7a$	0.951	5.705
(2) $A(^3D_2) + A(^1D_2) = b/12 + 2a$	0.222 + 0.32 (C)	
(3) $A(^3D_1) = -b/4 + 2a$	-1.414 (S)	5.656

From equations (1) and (3) $b = 5.704$ and $a = 0.006 \text{ cm}^{-1}$.

6s7d

Table II

Formula	Observed Interval Factors	b cms ⁻¹
(1) $A(^3D_3) = b/6 + 4/7a$	0.964	5.784
(2) $A(^3D_2) + A(^1D_2) = b/12 + 2a$	0.31(c) + 0.25 (c)	
(3) $A(^3D_1) = -b/4 + 2a$	-1.47 (c)	5.88

a represents the 7d electron.

From equations (1) and (3) is found $b = 5.816 \text{ cm}^{-1}$

$$a = -0.008 \text{ cm}^{-1}$$

6s8d

Table III

Formula	Observed Interval Factors	b cms ⁻¹
(1) $A(^3D_3) = b/6 + 4/7a$	0.99 (c)	5.94
(2) $A(^3D_2) + A(^1D_2) = b/12 + 2a$	0.66 (c)	
(3) $A(^3D_1) = -b/4 + 2a$	-1.50 (c)	6.00

a represents the 8d electron.

From equations (1) and (3) $b = 5.968 \text{ cms}^{-1}$

$$a = -0.004 \text{ cms}^{-1}$$

In applying the formulae to the observed structure of the states $6s6d$, $6s7d$ and $6s8d$ configurations, fairly consistent results are obtained. The values of a are derived from the formulae (1) and (3) since they involve terms independent of the coupling. The value of the term a is very small in comparison with the value of b , hence it may be neglected, resulting in the values shown for b in the third column of each table. In each table it is noticed that the values of b from equations (1) and (3) are in good agreement. Furthermore the value of b is seen to increase with increasing quantum number of the d electron, which may be explained as a decrease of the screening effect of the outer electrons on the inner $6s$ electron. The values of b obtained from equations (2) are not in very good agreement with those from equations (1) and (3).

6snf

s and f electron configurations give rise to the spectral states, represented as 3F_4 , 3F_3 , 1F_3 , and 3F_2 . These configurations are treated in tables IV and V in a manner similar to those of the $6snd$ configuration.

6s5f

Table IV

Formula	Observed Interval Factors	b cm ⁻¹
(1) $A(^3F_4) = b/8 + [2/3]d$	0.735 (c)	5.880
(2) $A(^3F_3) + A(^1F_3) = \frac{b}{24} + 2d$	-0.194(c) + 0.423(c)	
(3) $A(^3F_2) = -b/6 + 8d/5$	-0.996 (c)	5.976

d represents the 5f electron.

From equations (1) and (3) $b = 5.895 \text{ cm}^{-1}$
 $d = -0.003 \text{ ..}$

6s6f

Table V

Formula	Observed Interval Factors	b cm ⁻¹
$A(^3F_4) = b/8 + 2/3 d'$	0.782	6.256
$A(^3F_3) + A(^1F_3) = b/24 + 2d'$	-0.653 + 0.844	
$A(^3F_2) = -b/6 + 8d'/5$	-1.112	6.672

d' represents the 6f electron.

From equations (1) and (3) $b = 6.404 \text{ cm}^{-1}$
 $d = -0.025 \text{ ..}$

As in the 6snd configurations a fair agreement is found in the values of the interaction constant b, and the constants d and d' are of no appreciable value in comparison with b. It may also be noticed that as the quantum number of the f electron increases the value of b for the 6s electron increases.

6s7s and 6s9s

When for a two electron system, both electrons are in S-orbits, both may couple strongly with the nucleus and contribute appreciably to the splitting. Two equivalent s-electrons give rise to two spectral states 3S_1 and 1S_0 . The term 1S_0 exhibits no fine structure since its J value is zero. Since the nuclear spin quantum number I of thallium is one half, two hyperfine levels are found hence the state 3S_1 is split into two levels with F values of 3/2 and 1/2. The value of the interval factor $A(^3S_1)$ may be expressed as in equation (6) of the theory viz:

$$A(^3S_1) = \frac{1}{2} (a_{6s} + a_{9s})$$

McLennan and McLay and Crawford (15) made an estimate of 0.196 cm^{-1} for a_{9s} of Tl II, hence $a_{6s} = 5.870 \text{ cm}^{-1} - b$

They also found that $a_{7s} = 1.23 \text{ cm}^{-1}$

Table VI

Configuration	Term	$\text{cm}^{-1} \Delta$	$A \text{ cm}^{-1}$	$b \text{ cm}^{-1}$
6s9s	3S_1	4.549	3.033	5.870
6s7s	3S_1	4.980 (S)	3.320	5.410

A change of the values of b from 5.870 for the 6s electron to 0.196 for the 9s electron, indicates a rapid decrease in the coupling with the nucleus with increasing total quantum number. The higher value of b for the 6s9s configuration shows clearly how the

screening effect of the outer electron on the inner 6s electron decreases with increasing principal quantum number. However such a rapid change of values, is rather strange.

(jj) coupling

In tables VII, VIII, IX and X are shown the terms, the observed separation factors, and the values in terms of the factors for the individual electrons expected if the coupling were (jj). Since the coupling is not strictly (jj), only the summation relations will be considered in each case.

(a) 6s6d

Table VII

Term	A for (JJ) coupling	A observed
$6s_{\frac{1}{2}}6d_{\frac{1}{2}}^3 D_3$	$b/6 + 5/6 a'$	0.951
$6s_{\frac{1}{2}}6d_{\frac{1}{2}}^3 D_2$	$-b/6 + 7/6 a'$	0.222 (s)
$6s_{\frac{1}{2}}6d_{\frac{1}{2}}^1 D_2$	$b/4 + 3/4 a''$	0.32 (c)
$6s_{\frac{1}{2}}6d_{\frac{1}{2}}^3 D_1$	$-b/4 + 5/4 a''$	-1.414 (s)

S - Schuler's value

c - Crawford value

The symbols b, a' and a'' represent the separation factors of the 6s, $6d_{\frac{1}{2}}$ and $6d_{\frac{1}{2}}$ electrons respectively.

The summation relations result in the following equations :

$$A(^3D_3) + A(^3D_2) + A(^1D_2) + A(^3D_1) = 2(a' + a'')$$

$$A(^3D_3) + A(^3D_2) + A(^1D_2) = b/4 + 2a' + 3/4 a''$$

$$A(^3D_3) = b/6 + 5/6 a'$$

From these equations and the data of table VII, $a' + a'' = 0.039$ and 0.088 ; which are too widely different values to be of any reliability. Since the separation factor of the 3D_3 term is independent of coupling, and if the value $b = 5.704$ be taken, then a' is negligible. If the average value of $a' + a''$ be taken as 0.064 then $a'' = 0.064$.

6s7d

Table VIII

Term	A for (jj) coupling	A observed
$6s_{\frac{1}{2}} 7d_{\frac{3}{2}} {}^3D_3$	$b/6 + 5/6 a'$	0.964
$6s_{\frac{1}{2}} 7d_{\frac{3}{2}} {}^3D_2$	$-b/6 + 7/6 a'$	0.31 (c)
$6s_{\frac{1}{2}} 7d_{\frac{1}{2}} {}^1D_2$	$b/4 + \frac{3a''}{4}$	0.25 (c)
$6s_{\frac{1}{2}} 7d_{\frac{1}{2}} {}^3D_1$	$-b/4 + 5/4 a''$	-1.47 (c)

b , a' and a'' represent the $6s$, $7d_{\frac{3}{2}}$ and $7d_{\frac{1}{2}}$ electrons respectively.

Applying the summation relations,

$$A({}^3D_3) + A({}^3D_2) + A({}^1D_2) + A({}^3D_1) = 2(a' + a'')$$

$$A({}^3D_3) + A({}^3D_2) + A({}^1D_2) = b/4 + 2a' + [3/4]a''$$

$$A({}^3D_3) = b/6 + [5/6]a'$$

These equations give the values 0.027 and 0.104 for $a' + a''$. Substituting the value $b = 5.816$ in the expression for the term $A({}^3D_3)$, the value $a' = -0.006$ is found. Taking the average value of $a' + a'' = 0.065$ then $a'' = 0.071$

The values of $a' + a''$ are too widely different to be

of any appreciable weight.

6s5f

Table IX

Term	A for (jj) coupling	A observed
$6s_{\frac{1}{2}} 5f_{\frac{7}{2}} {}^3F_4$	$b/8 + [7/8]a'$	0.735 (c)
$6s_{\frac{1}{2}} 5f_{\frac{7}{2}} {}^3F_3$	$-\frac{b}{8} + \frac{9}{8}a'$	-0.194 (c)
$6s_{\frac{1}{2}} 5f_{\frac{5}{2}} {}^1F_3$	$\frac{b}{6} + \frac{5}{6}a''$	0.423 (c)
$6s_{\frac{1}{2}} 5f_{\frac{5}{2}} {}^3F_2$	$-\frac{b}{6} + \frac{7}{6}a''$	-0.996 (c)

b, a', a'' represent the $6s_{\frac{1}{2}} 5f_{\frac{7}{2}}$, $5f_{\frac{5}{2}}$ electrons respectively.

The summation relations lead to the following equations :

$$\begin{aligned}
 A({}^3F_4) + A({}^3F_3) + A({}^1F_3) + A({}^3F_2) &= 2(a' + a'') \\
 A({}^3F_4) + A({}^3F_3) + A({}^1F_3) &= \frac{b}{6} + 2a' + \frac{5a''}{6} \\
 A({}^3F_2) &= \frac{b}{8} + \frac{7a''}{8}
 \end{aligned}$$

Taking the value of $b = 5.995$, then since the term 3F_4 is independent of the coupling, the value of a' is found to be -0.002. From the above equations two values for $a' + a''$ are found to be -0.016 and -0.019 which are in good agreement, indicating that the term classification is correct. If the average value of $a' + a''$ be taken as -0.017 then $a'' = -0.015$.

6s6f

Table X

Term	A for (jj) coupling	A observed
$6s_{\frac{1}{2}} 6f_{\frac{7}{2}} {}^3F_4$	$\frac{b}{8} + \frac{7}{8} a'$	0.782
$6s_{\frac{1}{2}} 6f_{\frac{7}{2}} {}^3F_3$	$-\frac{b}{8} + \frac{9}{8} a'$	-0.653
$6s_{\frac{1}{2}} 6f_{\frac{5}{2}} {}^4F_3$	$\frac{b}{6} + \frac{5}{6} a''$	0.844
$6s_{\frac{1}{2}} 6f_{\frac{5}{2}} {}^3F_2$	$-\frac{b}{6} + \frac{7}{6} a''$	-1.112

b, a' and a'' represent the $6s_{\frac{1}{2}}$, $6f_{\frac{7}{2}}$ and $6f_{\frac{5}{2}}$ electrons respectively.

The separation factor of the term 3F_4 being independent of coupling, leads to a value of -0.021 for a' if b is taken to be 6.404 cm^{-1}

The summation relations lead to the following equations :-

$$\begin{aligned}
 A({}^3F_4) + A({}^3F_3) + A({}^4F_3) + A({}^3F_2) &= 2(a' + a'') \\
 A({}^3F_4) + A({}^3F_3) + A({}^4F_3) &= \frac{b}{6} + 2a' + \frac{5}{6} a'' \\
 A({}^3F_4) &= \frac{b}{8} + \frac{7}{8} a'
 \end{aligned}$$

These equations give the values -0.070 and -0.084 for a' + a'', which are in as close agreement as could be expected from the limits of accuracy of the data. The average value for a' + a'' may be taken as -0.077 then a'' = -0.056.

From the preceding discussion it may be concluded that the terms considered, do not belong to either the extreme (SL) coupling or (jj) coupling

The contribution of the non-^svalence electron to the interaction energy in each case may be regarded as negligible in comparison with the contribution of the valence s^{el}-electron.

Hyperfine structure analysis, besides revealing features of the interaction of the nucleus with the extra-nuclear electrons, constitutes a critical test of the correctness of the term classification. The classification is excellently confirmed if, for all the classified transitions, the observed hyperfine structure agrees with that predicted by attributing to each term, specific hyperfine structure intervals and F values. The present analysis confirmed all the previous classifications which were investigated.

Acknowledgments

I take this opportunity of thanking Professor Smith, whose guidance and help made this work possible. May I also extend my thanks to Mr. Gleave, whose co-operation and aid with respect to the apparatus, greatly facilitated the experimental procedure.

To all those who indirectly contributed to the production of this thesis, may I sincerely acknowledge my indebtedness.

References

- (1) S. Goudsmit and Humphrey - Phys. Rev. 31:960 (1928)
- (2) S. Goudsmit - Phys. Rev. 31:946 (1928)
- (3) L. Pauling & S. Goudsmit - Structure of Line spectra
- (4) E. Fermi - Zeits f. Physik - 60,320 (1930)
- (5) Casimir.
- (6) Hargreaves, Proc. Roy. Soc. A127, 141 (1930)
- (7) G. Breit, Phys. Rev. 37, 51 (1931)
- (8) S. Goudsmit - Phys. Rev. 37:663 (1931)
- (9) Goudsmit & Bacher - Phys. Rev. 34:1501 (1929)
- (10) Stanley Smith & J.S.Beggs- Can. Journ. Res. Vol.12:
690-698.1935.
- (11) Drude's Theory of Optics - page 391.
- (12) McLennan & McLeod - Proc. Roy. Soc. (London)
A.90:243-254. 1914.
- (14) Hill, Proc. Nat. Acad. Sci., 16, 68, 1930.
- (15) J.C. McLennan, McLay & Crawford - Proc. Roy. Soc.
vol. 133 p. 652 (1931)
- (16) K.R. Rao, A.L. Narayan, A.S. Rao, Indian Journ. Phys.2
page 467 (1928)
- (17) J.C. McLennan, A.B. McLay, M.F. Crawford, Trans.Roy.Soc.
Can. 22, p. 241 (1928)
- (18) S. Smith, Proc. Nat. Acad. Sci. 14, p.951 (1928)
- (19) McLennan, McLay, Crawford- Proc. Roy. Soc. A vol. 125
p. 570 (1929)
- (20) S. Smith - Phys. Rev; vol. 35, p. 235 (1930)
- (21) J.C. McLennan, M.F. Crawford, Proc. Roy. Soc., A vol.
132 p. 10 (1931)
- (22) Schuler, Keyston, Zeit f. Physik, 70 p.1. (1931)

THE SIGMA SENSITIVE RELAY

Types 1-A, 1-C

INSTRUCTIONS

MOUNTING

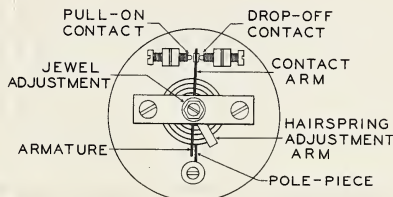
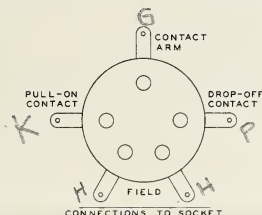
This relay is designed to be mounted in a standard five-prong tube socket, to the terminals of which the circuit connections are made, as indicated on the diagram. The polarity of the field terminals is optional.

ADJUSTMENTS

HAIRSPRING. For most purposes the best value of hairspring tension for a given field voltage and contact gap is obtained by the following procedure: Move the adjustment arm clockwise to a point at which the contact arm fails to swing across the gap between contacts when current is applied to the field. Then gradually move the adjustment arm back (counter-clockwise) somewhat past the point at which the magnet, when energized, can pull the contact arm across. At this adjustment the times consumed by pull-on and drop-off will be approximately equal.

CONTACTS. The gap between contacts may be varied to suit the user by turning the contact screws. When the gap is wide relay action is slower and requires more power than when the gap is narrow. The pull-on contact should always be so adjusted that when the field is energized the armature is pulled over close to, but never touching, the pole-piece. If the armature touches the pole-piece poor pull-on contacting is likely to result, as well as possible sticking of the movement.

PIVOT JEWEL. This should never need adjustment and should not be touched by one not skilled in the handling of jewelled bearings. We assume no responsibility for jewels damaged by inexpert manipulation.



INPUT POWER

The table below shows the voltages necessary to supply relays of different field resistances with four milliwatts (four thousandths of one watt) and the current, in milliamperes, which will be used at these voltages. The field resistance may be found on the serial number tag inside the relay. Voltages up to ten times these given in the table may be used with safety.

For Operation On Four Milliwatts					
Field Resistance Ohms	Input, D.C.		Field Resistance Ohms	Input, D.C.	
	Volts	Milliamperes		Volts	Milliamperes
17000.0	8.24	0.48	100.0	0.68	6.8
8750.0	5.19	0.76	25.0	0.81	12.4
1700.0	2.6	1.52	10.0	0.2	20.0
1000.0	2.0	2.0	2.5	0.1	40.0
250.0	1.0	4.0			

The following simple formulae will aid the untechnical in determining values:

$$\text{Volts} \times \text{Amperes} = \text{Watts}$$

$$\frac{\text{Volts}}{\text{Ohms}} = \text{Amperes}$$

CONTROL OF CURRENT

The hairspring will carry, and the contacts will control, up to one ampere of direct current, if sparking is kept at a minimum. High values of voltage, amperage, inductance or capacitance in the controlled circuit create sparking at the contacts. Direct current arcs more than alternating current does. The tendency of the contacts to weld together can be compensated for, if sparking is not too severe, by increasing the field input power and the hairspring tension. A resistance-capacity suppressor, in shunt with the working contacts, will eliminate or reduce sparking if the values of resistance and capacity have been well chosen to suit the conditions of the circuit. Excessive sparking, from whatever cause, is undesirable and will affect the operation of the relay.

WG. 11138-87 Ave.
31880

THE SIGMA SENSITIVE RELAY

Types 1-A, 1-C

INSTRUCTIONS

MOUNTING

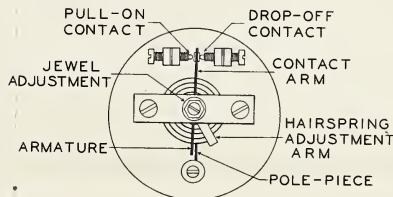
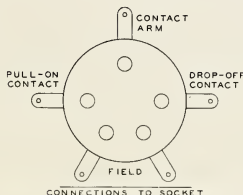
This relay is designed to be mounted in a standard five-prong tube socket, to the terminals of which the circuit connections are made, as indicated on the diagram. The polarity of the field terminals is optional.

ADJUSTMENTS

HAIRSPRING. For most purposes the best value of hairspring tension for a given field voltage and contact gap is obtained by the following procedure: Move the adjustment arm clockwise to a point at which the contact arm fails to swing across the gap between contacts when current is applied to the field. Then gradually move the adjustment arm back (counter-clockwise) somewhat past the point at which the magnet, when energized, can pull the contact arm across. At this adjustment the times consumed by pull-on and drop-off will be approximately equal.

CONTACTS. The gap between contacts may be varied to suit the user by turning the contact screws. When the gap is wide relay action is slower and requires more power than when the gap is narrow. The pull-on contact should always be so adjusted that when the field is energized the armature is pulled over close to, but never touching, the pole-piece. If the armature touches the pole-piece poor pull-on contacting is likely to result, as well as possible sticking of the movement.

PIVOT JEWEL. This should never need adjustment and should not be touched by one not skilled in the handling of jewelled bearings. We assume no responsibility for jewels damaged by inexperienced manipulation.



INPUT POWER

The table below shows the voltages necessary to supply relays of different field resistances with four milliwatts (four thousandths of one watt) and the current, in milliamperes, which will be used at these voltages. The field resistance may be found on the serial number tag inside the relay. Voltages up to ten times those given in the table may be used with safety.

For Operation On Four Milliwatts					
Field Resistance Ohms	Input, D.C.		Field Resistance Ohms	Input, D.C.	
	Volts	Milliamperes		Volts	Milliamperes
17000.0	8.24	0.48	100.0	0.63	6.8
8750.0	5.19	0.76	25.0	0.81	12.4
1700.0	2.6	1.52	10.0	0.2	20.0
1000.0	2.0	2.0	2.5	0.1	40.0
250.0	1.0	4.0			

The following simple formulae will aid the untechnical in determining values:

$$\text{Volts} \times \text{Amperes} = \text{Watts}$$

$$\frac{\text{Volts}}{\text{Ohms}} = \text{Amperes}$$

CONTROL OF CURRENT

The hairspring will carry, and the contacts will control, up to one ampere of direct current, if sparking is kept at a minimum. High values of voltage, amperage, inductance or capacitance in the controlled circuit create sparking at the contacts. Direct current arc more than alternating current does. The tendency of the contacts to weld together can be compensated for, if sparking is not too severe, by increasing the field input power and the hairspring tension. A resistance-capacity suppressor, in shunt with the working contacts, will eliminate or reduce sparking if the values of resistance and capacity have been well chosen to suit the conditions of the circuit. Excessive sparking, from whatever cause, is undesirable and will affect the operation of the relay.



872

Half-Wave Mercury-Vapor Rectifier

The RCA-872 is a half-wave, mercury-vapor rectifier tube of the hot-cathode type. It is intended for use in high-voltage devices designed to supply d-c power of uniform voltage. In single-phase circuits, full-wave rectification is accomplished by using two 872's.

CHARACTERISTICS

FILAMENT VOLTAGE	5.0	Volts
FILAMENT CURRENT	10	Amperes
PEAK INVERSE VOLTAGE:*		
For ambient temp. of 0° to 50°C	7500 max.	Volts
PEAK PLATE CURRENT	5.0 max.	Amperes
AVERAGE PLATE CURRENT (Averaged over 15 sec.)	1.25 max.	Amperes
TUBE VOLTAGE DROP (Approx.)	15	Volts
BULB (For dimensions, see page 6)	T-18	
CAP (For connection, see page 4)	Medium Metal	
BASE ** (For socket connections, see page 4)	Jumbo 4-Large Pin	

* For supply frequency up to 150 cycles.

** Base shell is not connected within base to either filament lead.

INSTALLATION

The base of the RCA-872 fits the standard, transmitting, four-contact socket, such as the RCA-type UT-541. The socket should be mounted so that the tube will operate in a vertical position with the base down.

The ambient temperature of the 872 should not be less than 0°C (32°F) and not more than 50°C (122°F). The ambient temperature is the temperature of the air which, coming into contact with the heated parts of the tube, carries off its heat. This temperature is to be measured by means of several thermometers placed at a distance of a few inches from the base. If the tube is used in a location where the circulation of air is restricted, the temperature should be taken adjacent to the filament base and with the thermometer shielded so that the effects of directly radiated heat are eliminated. If forced-air cooling is used, the ambient temperature is to be measured by a thermometer in the cooling-air stream before the air reaches the tube. The useful life of this tube may be seriously affected if the temperature range of operation is exceeded. Forced ventilation may be necessary to prevent exceeding the maximum allowable temperature under all conditions. In any case, adequate circulation of air is necessary and forced ventilation may be desirable from the standpoint of tube safety factor and life. When operated under load, RCA-872 has a characteristic blue glow. In service the bulb will eventually darken. This blackening is normal and is not an indication of the end of tube life.

The coated filament is intended for a-c operation from a secondary winding of a power transformer. This winding, provided with a center-tap or center-tap resistor, should supply at the socket terminals the rated voltage of 5.0 volts under average operating conditions. The filament voltage, measured at the tube terminals, should not vary more than plus or minus 5 per cent from the rated value. This tolerance should include the effects of regulation caused by transmitter-modulation load as well as the normal power-supply regulation. All connections in the filament circuit should be of low resistance and of adequate current-carrying capacity.

A filament voltmeter should be connected permanently across the filament circuit at the socket terminals so that the filament voltage can be maintained at 5.0 volts. *Caution should be observed when measuring filament voltage because the filament circuit is at high potential.*

When an RCA-872 is first placed in service, its filament should be operated at normal voltage for approximately 15 minutes without plate voltage in order to distribute the mercury properly. This procedure need not be repeated unless, during subsequent handling, mercury is spattered on the filament and plate.

The filament should always be allowed to come up to operating temperature before plate voltage is applied. Ordinarily, this may be accomplished by pre-heating the filament for 30 seconds. In radio transmitters during "standby" periods, the filament should be kept at its rated voltage to avoid delay in "coming back". If this is not done, the filament should always be pre-heated for approximately 30 seconds each time the plate voltage is applied.

Shields and r-f filter circuits should be provided for the 872 if it is subjected to extraneous high-voltage or high-frequency fields when in operation. These fields tend to produce breakdown effects in mercury vapor and are detrimental to tube life and performance. External shielding is employed when the tube is in proximity to high-voltage, high-frequency fields. R-f filters are employed to prevent damage caused by radio-frequency currents which might otherwise be fed back into the rectifier tube.

APPLICATION

As a single-phase or multi-phase rectifier, RCA-872 should be operated under conditions such that the maximum rated values under CHARACTERISTICS are not exceeded. Maximum Peak Inverse Voltage and Maximum Peak Plate Current are the fundamental limitations in the operation of this tube. See definitions, page 3.

Rectifier circuits particularly suited for use with the 872 are shown on page 5. A summary of the approximate conditions which can be obtained from the use of these circuits is shown in TABLE I. These values are based on sine-wave input and the use of a suitable choke preceding any condenser in the filter circuit. Each tabulated value of d-c voltage is the effective d-c output voltage from the rectifier

tube(s). Owing to the low tube-voltage drop of approximately 15 volts, the only reduction in rectified voltage when the load is increased is due to the drop in the transformer and filter windings. In the case of the single-phase full-wave (Fig. 2) and three-phase full-wave (Fig. 5) circuits, two 872's are used in series. These two circuits are desirable where higher d-c voltages are required. In the three-phase full-wave circuits, six-phase wave form is obtained.

Filter circuits of either the condenser-input or the choke-input type may be employed. If the condenser-input type of filter is used, special consideration must be given to the instantaneous peak value of the a-c input voltage which is about 1.4 times the RMS value as measured with an a-c voltmeter. It is important, therefore, that the filter condensers (especially the input condenser) have a sufficiently high breakdown rating to withstand this instantaneous peak value. With the condenser-input type of filter, the peak plate current of the tube is considerably higher than the load current. When choke input to the filter is used, the peak plate current is substantially reduced. This type of circuit is preferable from the standpoint of obtaining the maximum continuous d-c output current from the 872 under the most favorable conditions.

Maximum peak inverse voltage is the highest peak voltage that a rectifier tube can safely stand in the direction opposite to that in which it is designed to pass current. It is the safe arc-back limit with the tube operating within the specified temperature range. The relations between the peak inverse voltage, the d-c output voltage, and the RMS value of a-c input voltage, depend largely upon the individual characteristics of the rectifier circuit and the power supply. The presence of line surges, keying surges, or any other transient, or wave-form distortion may raise the actual peak voltage to a value higher than that calculated for sine-wave voltages. Therefore, the actual inverse voltage and not the calculated value should be such as not to exceed the rated maximum peak inverse voltage for the rectifier tube. A cathode-ray oscillograph or a spark gap connected across the tube is useful in determining the actual peak inverse voltage. In single-phase, full-wave circuits with sine-wave input, the peak inverse voltage on a rectifier tube is approximately 1.4 times the RMS value of the plate-to-plate voltage applied to the tube. In single-phase, half-wave circuits with sine-wave input and with condenser input to the filter, the peak inverse voltage may be as high as 2.8 times the RMS value of the applied plate voltage. In polyphase circuits, the peak inverse voltage must be calculated for the individual case.

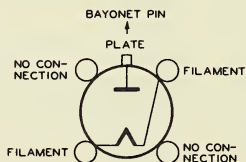
Maximum peak plate current is the highest peak current that a rectifier tube can safely stand in the direction in which it is designed to pass current. The safe value of this peak current in hot-cathode types of rectifiers is a function of the electron emission available and the duration of the pulsating current flow from the rectifier tube during each half cycle. In a given circuit, the value of peak plate current is largely determined by the filter constants. If a large choke is used in the filter circuit next to the rectifier tube(s), the peak plate current is not much greater than the load current; but if a large condenser is used in the filter next to the rectifier tube(s), the peak current is often many times the load current. In order to determine accurately the peak current in any circuit, the best procedure usually is to measure it with a peak-indicating meter or to use an oscillograph.

TABLE I *

CIRCUIT	MAXIMUM A-C INPUT VOLTS (RMS)	APPROX. D-C OUTPUT VOLTS TO FILTER	MAXIMUM D-C LOAD CURRENT AMPERES
SINGLE-PHASE FULL-WAVE (2 Tubes) Fig. 1	2650 per tube	2300	2.5
SINGLE-PHASE FULL-WAVE (4 Tubes) Fig. 2	5300 total	4750	2.5
THREE-PHASE HALF-WAVE (3 Tubes) Fig. 3	3050 per leg	3500	3.75
THREE-PHASE DOUBLE-Y PARALLEL (6 Tubes) Fig. 4	3050 per leg	3500	7.5
THREE-PHASE FULL-WAVE (6 Tubes) Fig. 5	3050 per leg	7000	3.75

* Based on a sine-wave input and the use of a suitable choke preceding any condenser in the filter circuit.

Tube Symbol and Top View of Socket Connections.



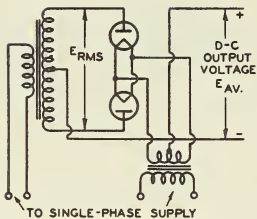


FIG. 1

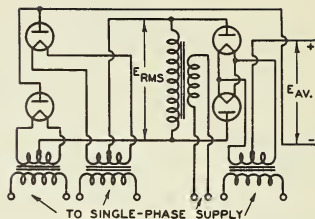


FIG. 2

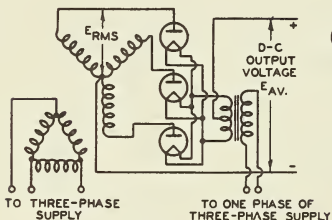


FIG. 3

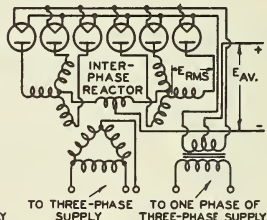


FIG. 4

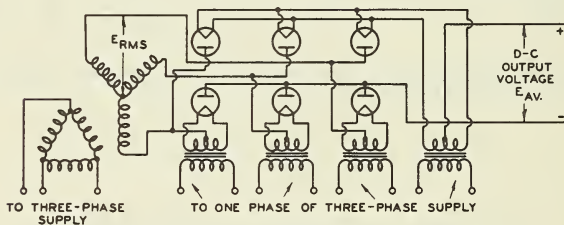


FIG. 5

FIGURE	CIRCUIT	E_{AVERAGE}	E_{INVERSE}	I_{AVERAGE}
1	SINGLE-PHASE FULL-WAVE (2 TUBES)	$0.318 E_{\text{MAXIMUM}}$ $0.450 E_{\text{RMS}}$	$3.14 E_{\text{AVERAGE}}$	$0.636 I_{\text{MAXIMUM}}$
2	SINGLE-PHASE FULL-WAVE (4 TUBES)	$0.636 E_{\text{MAXIMUM}}$ $0.900 E_{\text{RMS}}$	$1.57 E_{\text{AVERAGE}}$	$0.636 I_{\text{MAXIMUM}}$
3	THREE-PHASE HALF-WAVE	$0.827 E_{\text{MAXIMUM}}$ $1.170 E_{\text{RMS}}$	$2.09 E_{\text{AVERAGE}}$	$0.827 I_{\text{MAXIMUM}}$
4	THREE-PHASE DOUBLE-Y PARALLEL	$0.827 E_{\text{MAXIMUM}}$ $1.170 E_{\text{RMS}}$	$2.09 E_{\text{AVERAGE}}$	$1.91 I_{\text{MAXIMUM}}$
5	THREE-PHASE FULL-WAVE	$1.65 E_{\text{MAXIMUM}}$ $2.34 E_{\text{RMS}}$	$1.045 E_{\text{AVERAGE}}$	$0.955 I_{\text{MAXIMUM}}$

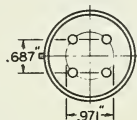
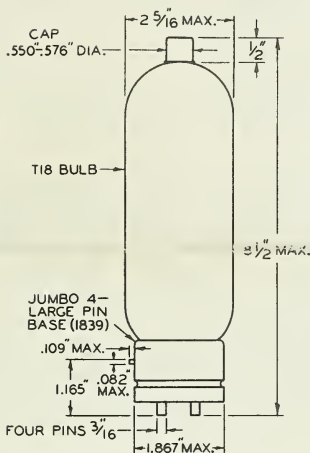
CONDITIONS ASSUMED :-

- (1) SINE-WAVE SUPPLY (2) BALANCED PHASE VOLTAGES (3) ZERO TUBE DROP
(4) PURE RESISTANCE LOAD (5) NO FILTER USED



872

OUTLINE DRAWING



BOTTOM VIEW OF BASE

92C-4323

